PAPER

Gram-scale synthesis of nitrogen doped graphene quantum dots for sensitive detection of mercury ions and L-cysteine†

Yuang Mao,‡[a] Chang Zhao,‡[a] Shuyan Ge,[b] Tao Luo,[a] Jie Chen,[a] Jiyang Liu, [ID] [b] Fengna Xi [ID] *[b] and Junjie Liu [ID] *[a]

Sensitive and reliable detection of mercury ions (Hg^{2+}) and L-cysteine (L-Cys) is of great significance for toxicology assessment, environmental protection, food analysis and human health. Herein, we present gram-scale synthesis of nitrogen doped graphene quantum dots (N-GQDs) for sensitive detection of Hg^{2+} and L-Cys. The N-GQDs are one-step synthesized using bottom-up molecular fusion in a hydrothermal process with gram-scale yield at a single run. N-GQDs exhibit good structural characteristics including uniform size (~2.1 nm), high crystallinity, and single-layered graphene thickness. Successful doping of N atom enables bright blue fluorescence (absolute photoluminescence quantum yield of 24.8%) and provides unique selectivity towards Hg^{2+}. Based on the fluorescence quenching by Hg^{2+} (turn-off mode), N-GQDs are able to serve as an effective fluorescent probe for sensitive detection of Hg^{2+} with low limit of detection (19 nM). As L-Cys could recover the fluorescence of N-GQDs quenched by Hg^{2+}, fluorescent detection of L-Cys is also demonstrated using turn-off-on mode.

1. Introduction

Metal ions and small biomarkers play crucial roles in various physiological and pathological processes.[1,2] For instance, mercury ions (Hg^{2+}) are one of the most toxic pollutants and are a great threat to the environment and human health. Even a small intake of Hg^{2+} (2 mg kg^{-1} body weight per day) can damage the nervous, endocrine and other systems, which further leads to many fatal diseases (*e.g.* headaches, renal failure, loss of intelligence quotient).[3–5] On the other hand, as one of the essential amino acids and small biomarkers in human body, L-cysteine (L-Cys) possesses vital physiological functions in neuronal tissues, metabolism and detoxication.[6–10] Abnormal levels of L-Cys can cause growth retardation, neurotoxic effect, Alzheimer's disease and coronary heart disease.[8–10] Therefore, simple and sensitive detection of Hg^{2+} and L-Cys is of great importance.

Up to now, many methods including atomic absorption spectrometry (AAS), atomic fluorescence spectrometry (AFS), inductively-coupled plasma mass spectrometry (ICP-MS) and surface-enhanced Raman scattering (SERS) have been

developed for the detection of Hg^{2+}.[1,11,12] However, these methods often require highly extensive instruments and sophisticated operation techniques. Several strategies including high performance liquid chromatography (HPLC) and capillary electrophoresis (CE) have been designed to detect L-Cys.[7,10] Tedious and time-consuming procedures are usually required. Among various detection techniques, fluorescence detections have attracted considerable interests owing to the ease of operation, rapid detection, high sensitivity, and possibility for real-time monitoring and local observation.[8,9,13,14] Until now, considerable efforts have been devoted to the development of fluorescent probes for monitoring Hg^{2+} or L-Cys.

Graphene quantum dots (GQDs) or 0D graphene are the newest addition to the nanocarbon family.[15–17] Owing to its atomic thickness, nanometer scale (<10 nm) and quantum confinement effect, GQDs exhibit tunable photoluminescence, high photostability, low cytotoxicity, and superior water dispersibility.[18,19] These unique properties promise a wide range of applications in biological imaging,[15,20] catalysis,[21–24] drug delivery,[19] energy conversion and storage[22,25] and especially sensing.[21,26–32] In recent years, it has been proved that heteroatom doping can effectively regulate the property and selectivity of GQDs. Challenge remains in facile and gram-scale synthesis of heteroatom-doped GQDs with specific selectivity.

In this work, we demonstrate gram-scale synthesis of nitrogen doped graphene quantum dots (N-GQDs) for sensitive detection of Hg^{2+} and L-Cys. As illustrated in Fig. 1, N-GQDs were easily synthesized through one-step bottom-up strategy under hydrothermal condition. The as-prepared N-GQDs show

[a] *Affiliated Tumor Hospital of Guangxi Medical University, 71 Hedi Road, Nanning 530021, PR China. E-mail: liujunjie186@163.com*

[b] *Department of Chemistry, Zhejiang Sci-Tech University, 928 Second Avenue, Xiasha Higher Education Zone, Hangzhou, 310018, PR China. E-mail: fengnaxi@zstu.edu.cn*

† Electronic supplementary information (ESI) available. See DOI: 10.1039/c9ra06113d
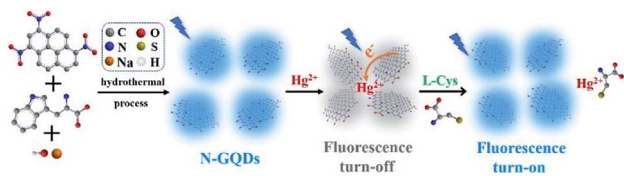
‡ The two authors contributed equally.

Fig. 1 Schematic illustration for the preparation of N-GQDs and detection of Hg^{2+} and L-Cys.

bright and emission-independent fluorescence, uniform size, and good crystalline. Owing to specific electron transfer and aggregation, N-GQDs exhibit selective and sensitive fluorescence quenching towards Hg^{2+}. In presence of L-Cys, the quenched fluorescence of N-GQDs/Hg^{2+} system could be recovered. Based on these fluorescence quenching (turn-off) and recovery (turn-off-on) processes, sensitive and simultaneous detection of Hg^{2+} and L-Cys are demonstrated.

2. Experimental

2.1 Materials and reagents

Pyrene, 4-(2-hydroxyethyl)-1-piperazineethanesulfonic acid (HEPES), NaOH, L-cysteine (L-Cys), L-histidine (His), D-methionine (Met), L-tryptophan, L-tyrosine (Tyr), L-leucine (Leu), L-threonine (Thr), L-alanine (Ala), L-glutamic acid (Glu), L-aspartic acid (Asp) and glycine (Gly) were obtained from Aladdin Chemistry Co. Ltd. (China). The standard solution of Hg^{2+} was purchased from National Standard Materials Center (China). Aqueous solutions of other cations were prepared from chloride salts (Ni^{2+}, K^+, Na^+, Ca^{2+}), nitrate salts (Zn^{2+}, Cr^{3+}, Ag^+, Co^{2+}, Cd^{2+}, Pb^{2+}, Fe^{3+}), and sulfate salts (Mg^{2+}, Cu^{2+}, Al^{3+}), respectively. All reagents are of analytical grade and used with further treatment. All aqueous solutions were prepared with ultrapure water (18.2 MΩ cm, Milli-Q, Millipore).

2.2 Characterizations

Transmission electron microscopic (TEM) images was taken on a JEM-2100 transmission electron microscope at operating voltage of 200 kV (JEOL Ltd., Japan). Atomic force microscopic (AFM) images were obtained using tapping mode by Bruker Multimode 8 (Bruker. Inc, USA). Elemental analysis of the N-GQDs was performed by X-ray photoelectron spectroscopy (XPS) with PHI5300 electron spectrometer (PE Ltd., USA) using Mg Kα radiation (250 W, 14 kV). Fluorescence spectra were recorded on RF-5301 PC spectrofluorometer (Shimadzu Corporation, Japan). Absolute photoluminescence quantum yield was measured using FL 3C-11 spectrofluorometer (Hariba Scientific, USA).

2.3 One-step preparation of N-GQDs

The precursor, 1,3,6-trinitropyrene, was synthesized according to the literature.[17] N-GQDs were prepared using one-pot hydrothermal process. Briefly, 1,3,6-trinitropyrene (6 mM) and L-tryptophan (75 mM) were dissolved in NaOH (125 mM) with ultrasonic treatment for 0.5 h. The mixture was then transferred into 500 mL Teflon-lined autoclave and heated for 6 h at 200 °C. To optimize the preparation conditions, different concentrations of L-tryptophan (25–120 mM) and NaOH (5 mM to 0.5 M), reaction temperature (120–200 °C) and time (2–10 h) were used. After the reaction, the obtained solution was filtered through a 0.22 μm microporous membrane to remove insoluble carbon product. N-GQDs could be obtained by freeze-drying after dialysis (retained molecular weight of 1000 Da) for 24 h to remove unreacted small molecules. The synthesis yield for N-GQDs was calculated based on the precursor.

2.4 Fluorescent turn-off detection of Hg^{2+}

The HEPES buffer solution (0.1 M, pH 6.0) containing tartaric acid (TA, 125 μM) was used for the detection of Hg^{2+}. N-GQDs (0.07 mg mL^{-1}) were mixed with Hg^{2+} at different concentrations (0.05–25 μM). After incubation at room temperature for 5 min, the fluorescence (FL) intensity in the absence (F_0) and presence (F) of Hg^{2+} was measured with the excitation wavelength fixed at 370 nm. The relative fluorescence ratio (F/F_0) and fluorescence quenching ratio ($F_0 - F$)/F_0 were used for calibration. Each detection was performed in triplicate.

For real sample analysis, the environmental sample was collected from Jinsha Lake (Hangzhou, China). Bacteria, algae and insoluble substances were removed by a 0.22 μm microporous membrane. The detection of Hg^{2+} was evaluated by standard addition method.

2.5 Fluorescence turn-off-on detection of L-Cys

As L-Cys can recover the fluorescence of N-GQDs quenched by Hg^{2+}, fluorescence turn-off-on mode was applied to detect L-Cys. Briefly, N-GQDs (0.07 mg mL^{-1}) was firstly mixed with Hg^{2+} (25 μM) and incubated for 5 min. Then, L-Cys was added at different concentrations (0.1–30.0 μM). After the mixed solution was incubated at room temperature for 5 min, the FL intensity was recorded (excited at 370 nm). The relative fluorescence recovery ratio ($F_1 - F$)/F_1 was used to evaluate the fluorescence recovery by L-Cys, where F and F_1 represent the FL intensity in absence and presence of L-Cys, respectively.

3. Results and discussion

3.1 Gram-scale synthesis of N-GQDs

In present work, N-GQDs were synthesized using one-step hydrothermal fusion between trinitropyrene and tryptophan in NaOH medium (Fig. 1). Trinitropyrene was chosen as precursor because it has the same mother-nucleus structure as graphene and could be fused at alkaline medium. Tryptophan with N atoms and carboxyl groups was applied as dopant to introduce doped heteroatoms as well as functional groups on GQDs. As demonstrated in inset of Fig. 2A, GQDs with blue fluorescence are obtained. In order to obtain GQDs with excellent fluorescent properties, the conditions of hydrothermal reaction were optimized. The highest fluorescence (FL) intensity is obtained at a reaction of 6 h and 200 °C (Fig. S1A and S1B†). Obviously, high temperature can facilitate the efficiency of the bottom-up fusion. However, higher temperature was not
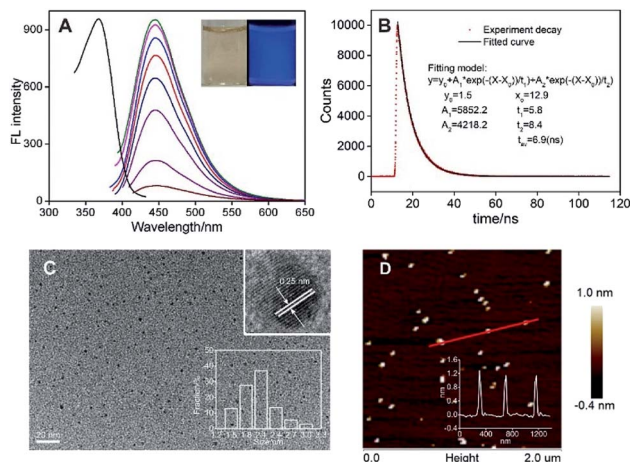
Fig. 2 (A) The FL excitation spectrum (EX, left) obtained at the emission wavelength of 445 nm and FL emission spectra (EM, right) of N-GQDs obtained with different excitation wavelength (340 to 410 nm, 10 nm increment). Insets are N-GQDs solution under daylight (left) and UV light (365 nm). (B) FL lifetime spectrum of N-GQDs. (C) TEM images of N-GQDs. Insets were the high-resolution TEM (HRTEM) image with indicated lattice parameter and size distribution of N-GQDs. (D) AFM image of the N-GQDs. Inset was the height profile along the red line.

investigated because it would have exceeded the tolerated range of the common Teflon-lined autoclave. Too short reaction time results in low concentration of GQDs due to incomplete molecule fusion, whereas too long time might result in GQDs stack. The FL intensity increases with the increase of tryptophan concentration and then reaches a plateau, presumably because the fusion between trinitropyrene and tryptophan is saturated (Fig. S1C†). The concentration of NaOH exhibits similar effects on the FL intensity of GQDs (Fig. S1D†). Thus, N-GQDs synthesized under the optimized conditions (75 mM L-tryptophan and 125 mM NaOH at 200 °C for 6 h) was applied for further investigation.

The synthesis yield of obtained N-GQDs is as high as 91.2%, indicating high efficiency for the preparation of N-GQDs. It is worth noting that the volume of the autoclave in present work is 500 mL, which is significantly higher than that used in most GQDs synthesis (usually 25 mL or 50 mL volume). Even the reaction solution is only 40% of the volume of autoclave, more than 0.5 g of N-GQDs could be produced at a single run. Thus, gram-scale synthesis of N-GQDs could be realized using this green and one-step strategy.

3.2 Fluorescence property, morphology and composition of N-GQDs

Fig. 2A demonstrates the fluorescent excitation and emission spectra of N-GQDs. As shown, the maximum excitation at 370 nm gives the maximum emission at 445 nm. It is worth noting that the maximum FL emission of N-GQDs remains unchanged when the excitation wavelength changes. In addition, a narrow emission is revealed with the half-peak width of about 55 nm (excited at 370 nm). These emission-independent and narrow emission suggest that N-GQDs have uniform

structure and luminescent states. The absolute quantum yield is 24.8% with a lifetime of 6.9 ns (Fig. 2B).

As revealed by transmission electron microscopy (TEM), the size of N-GQDs is uniform with average size of ~2.1 nm. The crystallinity of N-GQDs was confirmed by high resolution TEM (HRTEM). The lattice spacing of 0.25 nm corresponds to the graphene (100) planes (Fig. 2C). Good crystallinity of N-GQDs might be attributed to the trinitropyrene precursor (Fig. 1), which has the mother-nucleus structure as graphene. The atomic force microscopic (AFM) image shows that the thickness of N-GQDs is about 1.0 nm. Considering the doped heteroatoms and surface groups, the as-prepared N-GQDs are mostly single-layered (Fig. 2D). The uniform size, good crystalline and homogeneous thickness suggest excellent structure characteristics of N-GQDs, which also support the narrow and emission-independent fluorescence.

The composition of N-GQDs was investigated by X-ray photoelectron spectroscopy (XPS). XPS survey spectrum reveals the presence of C, O, and N with atomic percentages of 78.7%, 17.3% and 4.0%, respectively (Fig. 3A), indicating successful introduction of N atoms on GQDs. The high resolution C 1s spectrum clearly evidences the presence of C–C=C (sp^2 C, 284.6 eV), C–O/C–N (285.5 eV) and O–C=O (288.0 eV), respectively (Fig. 3B).[17] According to the high resolution O 1s spectrum, N-GQDs contains carboxyl group (532.8 eV) and hydroxyl group (531.4 eV) (Fig. 3C).[33] The pyrrole N (C–N–C, 398.7 eV) and graphite N (N–(C)$_3$, 399.2 eV) in high resolution N 1s spectrum indicate that N atoms have successfully doped into the carbon skeleton of GQDs.[34] In addition, N-GQDs also contain some primary amino groups (C–N–H, 400.1 eV) (Fig. 3D).

3.3 Selective fluorescence quenching of N-GQDs towards Hg^{2+}

The selectivity of N-GQDs towards different metal ions was investigated. As demonstrated in Fig. 4A, K$^+$, Na$^+$, Ca^{2+}, Mg^{2+},
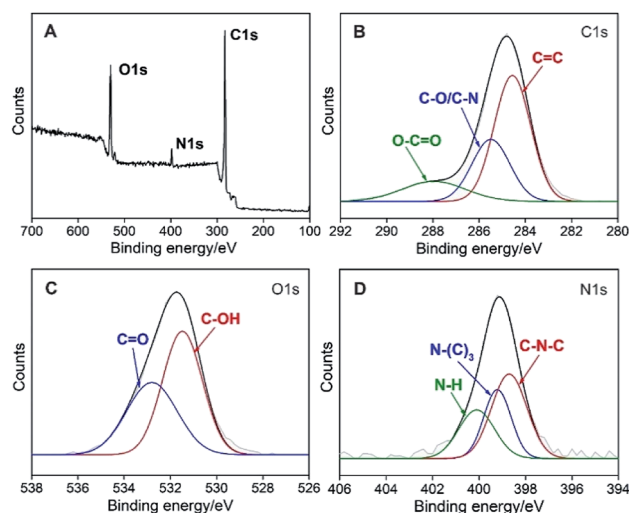

Fig. 3 XPS survey spectrum (A) and high resolution C 1s (B), O 1s (C), and N 1s (D) spectra of N-GQDs.
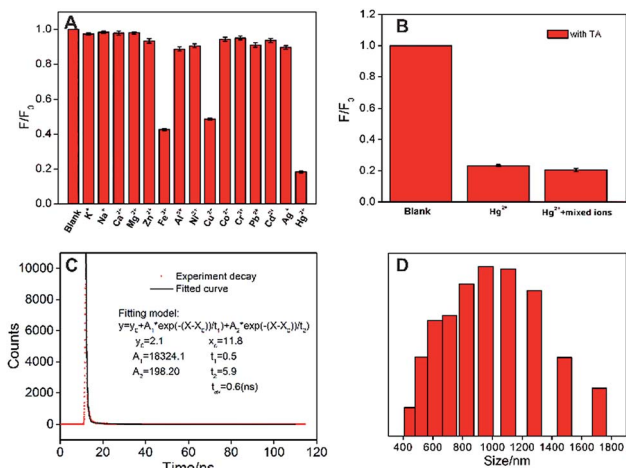
Fig. 4   (A) The relative FL ratio of the N-GQDs in the presence of different metal ions (25 μM). (B) The relative FL ratio of the N-GQDs in the presence of Hg^{2+} or Hg^{2+} + mixed ions (all other ions in A) with tartaric acid (TA, 125 μM). (C) FL lifetime spectrum of N-GQDs in the presence of Hg^{2+}. (D) The dynamic light scattering of N-GQDs in the presence of Hg^{2+}.
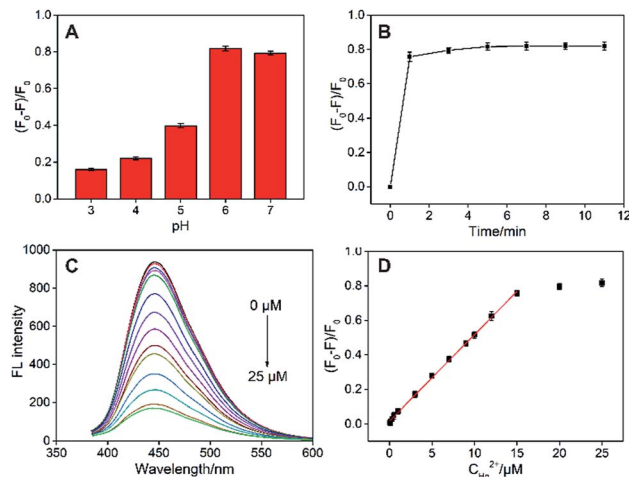

Fig. 5   (A) The relative FL ratio of N-GQDs with Hg^{2+} at different pH. (B) The effect of incubation time on fluorescent quenching ratio of N-GQDs caused by Hg^{2+} (25 μM). (C) FL emission spectra of N-GQDs in the presence of different concentrations of Hg^{2+}. (D) The linear dependence of $(F_0 - F)/F_0$ on concentration of Hg^{2+}.

Zn^{2+}, Al^{3+}, Ni^{2+}, Co^{2+}, Cr^{3+}, Pb^{2+}, Cd^{2+}, and Ag^+ hardly affect the fluorescence of N-GQDs. On the contrary, Hg^{2+}, Fe^{3+} and Cu^{2+} could quench the fluorescence of N-GQDs. However, the quenching efficiency of Hg^{2+} is significantly higher than that of Fe^{3+} and Cu^{2+}, indicating the potential for sensitive detection of Hg^{2+}. In contrast to most reported GQDs-based fluorescent sensors, which usually applied to detect Fe^{3+} or Cu^{2+}, GQDs with Hg^{2+} sensitivity is rarely reported. Tartaric acid (TA) is chosen as masking agent to eliminate the interference of Fe^{3+} and Cu^{2+}. As shown in Fig. S2,† the addition of TA has no effect on the fluorescence of N-GQDs. In the presence of TA (125 μM), the fluorescence of N-GQDs quenched by Hg^{2+} is similar with that obtained in mixture of Hg^{2+} and all other ions in Fig. 4A (Fig. 4B). Hence, selective fluorescence response of N-GQDs towards Hg^{2+} could be achieved.

The mechanism for the fluorescence quenching of N-GQDs by Hg^{2+} was investigated. Firstly, we measured the fluorescence lifetime of N-GQDs after interaction with Hg^{2+}. The lifetime of N-GQDs in presence of Hg^{2+} is 0.6 ns (Fig. 4C), which is remarkably shorter than that of N-GQDs itself (6.9 ns). This indicates fluorescence quenching by electron transfer between N-GQDs and Hg^{2+}, presumably because of the electron-donating moieties on GQDs formed by doped N atoms (Fig. 1). In addition, the remarkable change of particle size was also investigated by the dynamic light scattering (DLS). The average size of particles in N-GQDs-Hg^{2+} mixture is 1038.7 nm, indicating Hg^{2+}-induced aggregation of N-GQDs. (Fig. 4D). Thus, aggregation-induced-quenching also occurs (Fig. 1).

3.4   Fluorescent turn-off detection of Hg^{2+} using N-GQDs as fluorescent probes

Owning to selective fluorescence quenching by Hg^{2+}, fluorescent sensor (turn-off mode) was developed for the detection of Hg^{2+} using N-GQDs as fluorescent probe. To achieve the highest

sensitivity, the detection conditions including pH and incubation time were optimized. As shown in Fig. 5A, the highest fluorescence quenching exists at pH 6. Too low a pH value (pH 3–5) might weaken the interaction between N-GQDs and metal ions through protonation of N atoms on GQDs whereas too high a pH value (pH 7) possibly converts metal ions into hydroxide. At the same time, fast kinetics is observed and a plateau of fluorescence intensity appeared within 3 min (Fig. 5B), indicating the strong interaction between N-GQDs and Hg^{2+}. Under the optimized conditions, remarkable decrease in FL intensity towards different concentration of N-GQDs is observed (Fig. 5C). Good linearity existed between fluorescent quenching ratio $(F_0 - F)/F_0$ and Hg^{2+} concentration from 50 nM to 15 μM (Fig. 5D). The limit of detection (LOD) is 19 nM at a signal-to-noise ratio of 3. As shown in Table S1 (ESI†), the detection limit obtained with the present method was lower than those obtained by carbon dots (CDs),[35] F doped CDs (F-CDs),[36] N doped CDs (N-CDs),[37] N and S co-doped CDs (N, S-CDs),[38,39] N doped GQDs (N-GCDs),[34] sulfur and nitrogen co-doped GQDs (S,N-GQDs),[40] and N-GQDs,[41] but higher than that obtained using Rhodamine B assisted GQDs (RhB-GQDs)[42] and N and S co-doped GQDs (N, S-GQDs).[43]

The application of the as-prepared fluorescent sensor for detection of Hg^{2+} in environmental samples (lake water) was

Table 1   Detection of Hg^{2+} in environmental water samples

Sample	Concentration of (μM)		RSD ($n = 3$, %)	Recovery (%)
	Added Hg^{2+}	Found by N-GQDs		
1	3.00	2.91, 2.83, 2.96	2.2	96.7
2	7.00	6.72, 6.65, 6.88	1.8	96.4
3	12.0	11.6, 11.9, 12.0	1.7	98.6

investigated (Table 1). As the original Hg^{2+} is not detected, the standard addition method was applied to evaluate the detection reliability. Good recoveries ranged from 96.4% to 98.6% were obtained, indicating the potential application of N-GQDs in real analysis.

3.5 Detection of L-Cys based on fluorescent off-on mode

As illustrated in Fig. 6A, the fluorescence of N-GQDs quenched by Hg^{2+} could be recovered after addition of L-Cys to the N-GQDs-Hg^{2+} system. As shown in Fig. 6B, L-Cys itself has no effect on the fluorescence intensity of N-GQDs. The possible interference of other nine common amino acids on the detection of L-Cys was investigated. As shown in Fig. 6A, these amino acids could not significantly restore the fluorescence of N-GQDs quenched by Hg^{2+}, indicating good selectivity of L-Cys. We speculate that the fluorescence recovery by L-Cys is due to the specific binding between –SH and Hg^{2+}. In support of this notion, glutathione (GSH, tripeptide composed of Cys, glycine, and glutamic acid) and homocysteine (Hcy, only include an additional $-CH_2-$ before –SH in comparison with Cys) also recover the fluorescence to some extent because of the similar structure as Cys (Fig. S3†). Fluorescence turn-off-on sensing mode could be developed for individual detection of L-Cys as a proof-of-demonstration. As shown in Fig. 6C, the fluorescence of N-GQDs gradually restores with increasing the concentration of L-Cys. Good linear relationship is found between fluorescence recovery rate and the concentration of L-Cys from 100 nM to 50 μM (DL of 29 nM) (Fig. 6D). As shown in Table S2,† the detection limit obtained with the present method was lower than those obtained by N,S-CDs-Fe^{3+},[44] N-CDs-Hg^{2+},[47] Eu-GQDs-Cu^{2+},[48] and N-GQDs-Hg^{2+},[49] but higher than that obtained using CDs-Hg^{2+},[45] N-CDs@V_2O_5,[46] and N-GQDs-Hg^{2+}.[49] The application of the N-GQDs-Hg^{2+} system for detection of L-Cys in environmental

samples (lake water) was investigated using standard addition method (Table S3†). Good recoveries ranged from 94.1% to 97.8% were obtained.

4. Conclusions

Gram-scale synthesis of nitrogen doped graphene quantum dots (N-GQDs) with Hg^{2+} sensitivity was readily achieved using one-step hydrothermal process. Such blue N-GQDs exhibit good characteristics including uniform size, good crystalline, bright and emission-independent fluorescence and single-layered graphene thickness. The ability to interact with Hg^{2+} results in selective and sensitive fluorescence quenching through electron transfer and aggregation. With N-GQDs being fluorescent probes, turn-off sensing of Hg^{2+} and turn-off-on detection of L-cysteine were demonstrated. The easy preparation and good characteristics of N-GQDs promise a large variety of applications, including optical sensing, photocatalysis and bioimaging.

Conflicts of interest

There are no conflicts to declare.

Acknowledgements

References

1 H. N. Kim, W. X. Ren, J. S. Kim and J. Yoon, Fluorescent and colorimetric sensors for detection of lead, cadmium, and mercury ions, *Chem. Soc. Rev.*, 2012, **41**, 3210–3244.

2 M. Gao, X. Lu, S. Chen, D. Tian, Y. Zhu and C. Wang, Enhanced peroxidase-like activity of Mo^{6+}-doped Co_3O_4 nanotubes for ultrasensitive and colorimetric L-cysteine detection, *ACS Appl. Nano Mater.*, 2018, **1**, 4703–4715.

3 Y. Liu, Y. Deng, T. Li, Z. Chen, H. Chen, S. Li and H. Liu, Aptamer-based electrochemical biosensor for mercury ions detection using AuNPs-modified glass carbon electrode, *J. Biomed. Nanotechnol.*, 2018, **14**, 2156–2161.

4 S. Y. Ding, M. Dong, Y. W. Wang, Y. T. Chen, H. Z. Wang, C. Y. Su and W. Wang, Thioether-based fluorescent covalent organic framework for selective detection and facile removal of mercury(II), *J. Am. Chem. Soc.*, 2016, **138**, 3031–3037.

5 G. H. Chen, W. Y. Chen, Y. C. Yen, C. W. Wang, H. T. Chang and C. F. Chen, Detection of mercury(II) ions using colorimetric gold nanoparticles on paper-based analytical devices, *Anal. Chem.*, 2014, **86**, 6843–6849.

6 M. Gao, X. Lu, M. Chi, S. Chen and C. Wang, Fabrication of oxidase-like hollow $MnCo_2O_4$ nanofibers and their sensitive
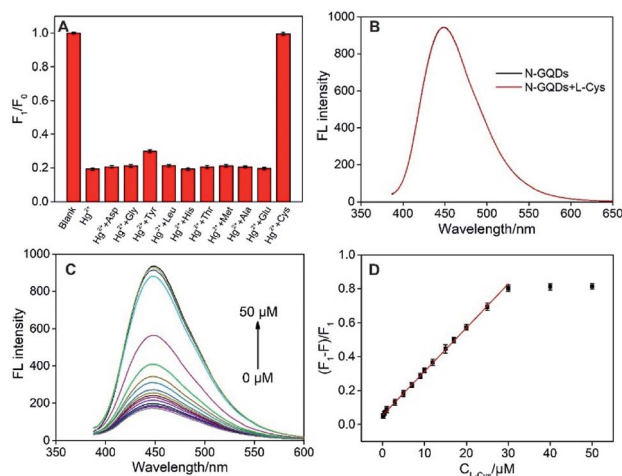
Fig. 6 (A) The relative FL ratio of N-GQDs with Hg^{2+} in the presence of different amino acid. (B) FL emission spectra of N-GQDs in the absence and presence of L-Cys (50 μM). (C) FL emission spectra of N-GQDs with Hg^{2+} (25 μM) in the presence of different concentrations of L-Cys. (D) The linear dependence of $(F_1 − F)/F_1$ on concentration of L-Cys.

colorimetric detection of sulfite and L-cysteine, *Inorg. Chem. Front.*, 2017, **4**, 1862–1869.

7 H. Li, L. Ye, Y. Wang and C. Xie, A glassy carbon electrode modified with hollow cubic cuprous oxide for voltammetric sensing of L-cysteine, *Microchim. Acta*, 2018, **185**, 5.

8 X. Li, X. Y. Yang, J. Q. Sha, T. Han, C. J. Du, Y. J. Sun and Y. Q. Lan, POMOF/SWNT nanocomposites with prominent peroxidase-mimicking activity for L-cysteine "on-off switch" colorimetric biosensing, *ACS Appl. Mater. Interfaces*, 2019, **11**, 16896–16904.

9 Y. C. Liang, Q. Zhao, X. Y. Wu, Z. Li, Y. J. Lu, Q. Liu, L. Dong and C. X. Shan, A ratiometric fluorescent nanoprobe based on quenched carbon dots-rhodamine B for selective detection of L-cysteine, *J. Alloys Compd.*, 2019, **788**, 615–622.

10 Y. Zhu, Z. Xu, K. Yan, H. Zhao and J. Zhang, One-Step Synthesis of $CuO-Cu_2O$ heterojunction by flame spray pyrolysis for cathodic photoelectrochemical sensing of L-cysteine, *ACS Appl. Mater. Interfaces*, 2017, **9**, 40452–40460.

11 J. Wu, P. Ran, S. Zhu, F. Mo, C. Wang and Y. Fu, A highly sensitive electrochemiluminescence sensor for the detection of L-cysteine based on the rhombus-shaped rubrene microsheets and platinum nanoparticles, *Sens. Actuators, B*, 2019, **278**, 97–102.

12 Y. Guo, Z. Wang, H. Shao and X. Jiang, Hydrothermal synthesis of highly fluorescent carbon nanoparticles from sodium citrate and their use for the detection of mercury ions, *Carbon*, 2013, **52**, 583–589.

13 P. Makam, R. Shilpa, A. E. Kandjani, S. R. Periasamy, Y. M. Sabri, C. Madhu, S. K. Bhargava and T. Govindaraju, SERS and fluorescence-based ultrasensitive detection of mercury in water, *Biosens. Bioelectron.*, 2018, **100**, 556–564.

14 F. Yan, Y. Zou, M. Wang, X. Mu, N. Yang and L. Chen, Highly photoluminescent carbon dots-based fluorescent chemosensors for sensitive and selective detection of mercury ions and application of imaging in living cells, *Sens. Actuators, B*, 2014, **192**, 488–495.

15 Y. Yan, J. Gong, J. Chen, Z. Zeng, W. Huang, K. Pu, J. Liu and P. Chen, Recent advances on graphene quantum dots: From chemistry and physics to applications, *Adv. Mater.*, 2019, **31**, e1808283.

16 Y. Du and S. Guo, Chemically doped fluorescent carbon and graphene quantum dots for bioimaging, sensor, catalytic and photoelectronic applications, *Nanoscale*, 2016, **8**, 2532–2543.

17 L. Wang, Y. Wang, T. Xu, H. Liao, C. Yao, Y. Liu, Z. Li, Z. Chen, D. Pan, L. Sun and M. Wu, Gram-scale synthesis of single-crystalline graphene quantum dots with superior optical properties, *Nat. Commun.*, 2014, **5**, 5357.

18 S. Zhu, Y. Song, J. Wang, H. Wan, Y. Zhang, Y. Ning and B. Yang, Photoluminescence mechanism in graphene quantum dots: Quantum confinement effect and surface/edge state, *Nano Today*, 2017, **13**, 10–14.

19 X. Yao, X. Niu, K. Ma, P. Huang, J. Grothe, S. Kaskel and Y. Zhu, Graphene quantum dots-capped magnetic mesoporous silica nanoparticles as a multifunctional platform for controlled drug delivery, magnetic hyperthermia, and photothermal therapy, *Small*, 2017, **13**, 1602225.

20 J. Dong, K. Wang, L. Sun, B. Sun, M. Yang, H. Chen, Y. Wang, J. Sun and L. Dong, Application of graphene quantum dots for simultaneous fluorescence imaging and tumor-targeted drug delivery, *Sens. Actuators, B*, 2018, **256**, 616–623.

21 Y. Yan, J. Chen, N. Li, J. Tian, K. Li, J. Jiang, J. Liu, Q. Tian and P. Chen, Systematic bandgap engineering of graphene quantum dots and applications for photocatalytic water splitting and CO_2 reduction, *ACS Nano*, 2018, **12**, 3523–3532.

22 J. Tian, J. Chen, J. Liu, Q. Tian and P. Chen, Graphene quantum dot engineered nickel-cobalt phosphide as highly efficient bifunctional catalyst for overall water splitting, *Nano Energy*, 2018, **48**, 284–291.

23 F. Xi, J. Zhao, C. Shen, J. He, J. Chen, Y. Yan, K. Li, J. Liu and P. Chen, Amphiphilic graphene quantum dots as a new class of surfactants, *Carbon*, 2019, **153**, 127–135.

24 Z. Zeng, F. Xiao, H. Phan, S. Chen, Z. Yu, R. Wang, T. Nguyen and T. Tan, Unraveling the cooperative synergy of zero-dimensional graphene quantum dots and metal nanocrystals enabled by layer-by-layer assembly, *J. Mater. Chem. A*, 2018, **6**, 1700–1713.

25 Q. Wang, Z. Jin, D. Chen, D. Bai, H. Bian, J. Sun, G. Zhu, G. Wang and S. F. Liu, μ-Graphene crosslinked $CsPbI_3$ quantum dots for high efficiency solar cells with much improved stability, *Adv. Energy Mater.*, 2018, **8**, 1800007.

26 C. Shen, S. Ge, Y. Pang, F. Xi, J. Liu, X. Dong and P. Chen, Facile and scalable preparation of highly luminescent N,S co-doped graphene quantum dots and their application for parallel detection of multiple metal ions, *J. Mater. Chem. B*, 2017, **5**, 6593–6600.

27 S. Bian, C. Shen, Y. Qian, J. Liu, F. Xi and X. Dong, Facile synthesis of sulfur-doped graphene quantum dots as fluorescent sensing probes for Ag^+ ions detection, *Sens. Actuators, B*, 2017, **242**, 231–237.

28 D. Chen, X. Zhuang, J. Zhai, Y. Zheng, H. Lu and L. Chen, Preparation of highly sensitive Pt nanoparticles-carbon quantum dots/ionic liquid functionalized graphene oxide nanocomposites and application for H_2O_2 detection, *Sens. Actuators, B*, 2018, **255**, 1500–1506.

29 B. Y. Fang, C. Li, Y. Y. Song, F. Tan, Y. C. Cao and Y. D. Zhao, Nitrogen-doped graphene quantum dot for direct fluorescence detection of Al^{3+} in aqueous media and living cells, *Biosens. Bioelectron.*, 2018, **100**, 41–48.

30 S. Bian, C. Shen, H. Hua, L. Zhou, H. Zhu, F. Xi, J. Liu and X. Dong, One-pot synthesis of sulfur-doped graphene quantum dots as a novel fluorescent probe for highly selective and sensitive detection of lead(II), *RSC Adv.*, 2016, **6**, 69977–69983.

31 L. Lu, L. Zhou, J. Chen, F. Yan, J. Liu, X. Dong, F. Xi and P. Chen, Nanochannel confined graphene quantum dots for ultrasensitive electrochemical analysis of complex samples, *ACS Nano*, 2018, **12**, 12673–12681.

32 J. Ju, R. Zhang and W. Chen, Photochemical deposition of surface-clean silver nanoparticles on nitrogen-doped graphene quantum dots for sensitive colorimetric detection of glutathione, *Sens. Actuators, B*, 2016, **228**, 66–73.

33 Q. Xiao, S. Lu, C. Huang, W. Su and S. Huang, Novel N-doped carbon dots/beta-cyclodextrin nanocomposites for enantioselective recognition of tryptophan enantiomers, *Sensors*, 2016, **16**, 1874.

34 Z. Yan, X. Qu, Q. Niu, C. Tian, C. Fan and B. Ye, A green synthesis of highly fluorescent nitrogen-doped graphene quantum dots for the highly sensitive and selective detection of mercury(II) ions and biothiols, *Anal. Methods*, 2016, **8**, 1565–1571.

35 H. Goncalves, A. Duarte and J. Silva, Optical fiber sensor for Hg (II) based on carbon dots, *Biosens. Bioelectron.*, 2010, **26**, 1302–1306.

36 Z. Gao, Z. Lin, X. Chen, Z. Lai and Z. Huang, Carbon dots-based fluorescent probe for trace Hg^{2+} detection in water sample, *Sens. Actuators, B*, 2016, **222**, 965–971.

37 R. Zhang and W. Chen, Nitrogen-doped carbon quantum dots: Facile synthesis and application as a "turn-off" fluorescent probe for detection of Hg^{2+} ions, *Biosens. Bioelectron.*, 2014, **55**, 83–90.

38 Y. Wang, S. Kim and L. Feng, Highly luminescent N, S-co-doped carbon dots and their direct use as mercury (II) sensor, *Anal. Chim. Acta*, 2015, **890**, 134–142.

39 L. Li, B. Yu and T. You, Nitrogen and sulfur co-doped carbon dots for highly selective sensitive detection of Hg (II) ions, *Biosens. Bioelectron.*, 2015, **74**, 263–269.

40 E. Sharma, D. Vashisht, A. Vashisht, V. Vats, S. Mehta and K. Singh, Facile synthesis of sulfur and nitrogen codoped graphene quantum dots for optical sensing of Hg and Ag ions, *Chem. Phys. Lett.*, 2014, **55**, 83–90.

41 Y. Liu, X. Tang, M. Deng, Y. Cao, Y. Li, H. Zhang, F. Li, F. Yan, T. Lan, L. Shi, L. Gao, L. Huang, T. Zhu, H. Lin, Y. Bai, D. Qu, X. Huang and F. Qiu, Nitrogen doped graphene quantum dots as a fluorescent probe for mercury(II) ions, *Microchim. Acta*, 2019, **186**, 140–147.

42 Y. Yang, X. Xiao, X. Xing, Z. Wang, T. Zou, Z. Wang, R. Zhao and Y. Wang, Rhodamine B assisted graphene quantum dots flourescent sensor system for sensitive recognition of mercury ions, *J. Lumin.*, 2019, **207**, 273–281.

43 N. Anh, A. Chowdhury and R. Doong, Highly sensitive and selective detection of mercury ions using N, S-codoped graphene quantum dots and its paper strip based sensing application in wastewater, *Sens. Actuators, B*, 2017, **252**, 1169–1178.

44 H. Wu, J. Jiang, X. Gu and C. Tong, Nitrogen and sulfur co-doped carbon quantum dots for highly selective and sensitive fluorescent detection of Fe (III) ions and L-cysteine, *Microchim. Acta*, 2017, **184**(7), 2291–2298.

45 F. Yan, D. Shi, T. Zheng, K. Yun and X. Zhou, Carbon dots as nanosensor for sensitive and selective detection of Hg^{2+} and L-Cysteine by means of fluorescence "Off-On" switching, *Sens. Actuators, B*, 2016, **224**, 926–935.

46 A. B. Ganganboina, A. C. Dutta and R. A. Doong, N-doped graphene quantum dots-decorated V_2O_5 nanosheet for fluorescence turn off-on detection of cysteine, *ACS Appl. Mater. Interfaces*, 2018, **10**, 614–624.

47 H. Huang, Y. Weng, L. Zheng, B. Yao, W. Weng and X. Lin, Nitrogen-doped carbon quantum dots as fluorescent probe for "off-on" detection of mercury ions, L-cysteine and iodide ions, *J. Colloid Interface Sci.*, 2017, **506**, 373–378.

48 L. Lin, X. Song, Y. Chen, M. Rong, Y. Wang, L. Zhao, T. Zhao and X. Chen, Europium-decorated graphene quantum dots as a fluorescent probe for label-free, rapid and sensitive detection of Cu^{2+} and L-cysteine, *Anal. Chim. Acta*, 2015, **891**, 261–268.

49 Z. Liu, Y. Gong and Z. Fan, Cysteine detection using a high-fluorescence sensor based on a nitrogen-doped graphene quantum dot-mercury(II) system, *J. Lumin.*, 2016, **175**, 129–134.